SUPPLEMENTAL INFORMATION

Assumption of steady state flux

Here we present results of simulations of one-dimensional topography to assess the quality of our assumption of steady state used to model slope as a continuous function of topographic position (Figure 2 of the main text). We find that while the study hillslope may not be in an absolute steady state, fluxes are still likely to vary with the distance (or drainage area per contour length in 2D) in a nearly linear manner, as predicted by the steady-state approximation. To compare real and simulated topographies we define a dimensionless quantity E^* (Fig. S3A).

In the range of E^* values similar to those of the study area (~1.2), slopes are only 60 – 80% of steady state slopes (Fig. S3 B, C). However, they are relatively consistent about this value (particularly in the non-linear case) suggesting that in this transient setting the degree of misestimation of flux does not vary significantly along the hillslope. In other words, while these landscapes may not be in steady state, flux still varies linearly with upstream area as it would in a steady state world. Our use of this approach is targeted at identifying discrepancies in flux that would arise at the abrupt, local changes in slope associated with shadow bedding. Therefore, we feel that the fact that this mis-estimation is consistent along the length of the modelled hillslopes justifies the use of the equilibrium-modeled slopes to develop the desired continuous function.

SUPPLEMENTAL FIGURE CAPTIONS

Table 1. Summary of data compiled and shown in Figure 3. ID corresponds to the legend shown in Figure 3 A. Measurement ID refers to the sample or location number in the publication. Maximum value gives the units and value used to normalize each data set. When appropriate, we specify either the species studied or the duration of the measurement interval over which creep rates or distances were measured.

Figure S1. Additional field photos documenting shadow bedding from the Northern Gabilan Mesa. **A)** East facing panorama taken overlooking Pine Valley Road highlighting both the upper surface of the Gabilan Mesa and shadow bedding. Note that shadow beds can be correlated for a long distance along hillslopes and in some cases across valleys. Also note that shadow beds are just as well expressed on hillslopes whose divides have lowered substantially below the mesa surface. **B)** Extended Panaroma of the same hillslope photographed in Figure 1 of the main text. Photo is taken facing East. **C)** Shadow bedding is seen on hillslopes in the foreground and background of this South Facing Photo. Pancho Rico Creek forms the valley in the midground of the photo. In the foreground, shadow bedding is partially highlighted by variations in vegetation.

Figure S2. Composite stratigraphic section from two sections measured at nearly equivalent stratigraphic positions in the Pancho Rico Formation. Sections were correlated based on the resistant, bioclastic conglomerate unit 16 m from the base of the displayed section. The expected location of this conglomerate in the landscape is shown

in Figure 1, and was computed by least-squares fitting of a plane to the surveyed basal contact of this bed. Dotted outlines of stratigraphy indicate beds that could not be accessed directly in one section and were partly soil mantled in the other. Measurements of thickness in these top beds were made from photographs, theodolite, GPS surveys and grain-size profiles were partly inferred from weathering profiles and based on limited outcrop access. Grain sizes are reported for the matrix, scale is labelled as mud (md), very-fine lower and upper sand (vfL and vfU), fine lower and fine upper sand (fL and fU), and medium lower sand (mL). Shell and rare pebble clasts are seen in beds near the middle of the section. In the two thin beds between 14 and 16 meters, long axis of clasts are typically 1-2 cm in diameter. In the thicker bed, fossil clasts are typically ~5 – 10 cm and in some cases even larger.

Figure S3. Transient slope evolution of linear and non-linear hillslopes. **A)** Depiction of terms used to compare real and modeled landscapes. Solid line depicts hillslope, dashed line shows the total uplift that has accrued or, alternatively, an incised landscape surface. E^* depends on the degree to which hillslopes have evolved beyond their initial condition and may be defined in the field utilizing an incised but relatively continuous geomorphic surface (the 'mesa' of the Gabilan Mesa). The two presented equations for E^* may be used to calculate this value in different circumstances. In the field, direct measurements of the hillslope relief, R_{hs}, and the incised surface relief, R_{surf}, can be made. In simulations, the equivalent quantities are the elevation of the hillslope crest, Z_{crest}, and the product of the uplift rate, u, and the model time, t. Relief is defined relative to the elevation at the base of the hillslope. The crest of the hillslope studied here is

approximately 20 – 30 m below the low-relief mesa surface and has ~100m of relief, suggesting it has an E^* value of ~1.2. **B and C)** Plots of the steady-state slope, S_{ss}, plotted against the slope at a specified simulation time, S_i, for different values of E^*. In **B** this is shown for a system evolving according to a linear transport rule, while in **C** the simulation was governed by a non-linear transport rule, as indicated by the titles of each plot. Dashed lines are contours of current slopes being 100%, 80% and 60% of equilibrium slopes.

TABLE 1

ID	Publication			Maximum Value	
Trees		***Measurement ID***	***Species***		
1	Danion et al., 1999	Oak 1	Sessile oak, *Quercus petraea*	2.81E+03	cm^3
2		Oak 2	Sessile oak, *Quercus petraea*	6.59E+02	cm^3
3		Oak 3	Sessile oak, *Quercus petraea*	2.59E+02	cm^3
4		Pine	Mean of 30*x* Maritime pine, *Pinus pinaster*	1.91E+02	cm^3
5	Danjon et al., 2008	Tree D	White oak, Quercus *alba*	1.11E+03	cm^2
6		Tree S	White oak, *Quercus alba*	2.83E+02	cm^2
7	Roering et al., 2010	Pine	Douglas fit, *Pseudotsuga menziesii*	5.30E-03	Root-soil area ratio
Burrowers		***Measurement type***			
8	Grinnell and Dixon, 1918	Burrow Area (from 3 sketches)	Ground squirrel, *Otospermophilus beecheyi*	6.21E+03	cm^2
9	Kolb, 1985	Burrow Area (from sketch)	European rabbit, *Oryctolagus cuniculus*	7.23E+02	cm^2
10	Miller, 1957	Burrow Volume	Pocket gopher, *Thomomys umbrinus*	5.23E+05	cm^3
11	Yensen et al., 1991	Burrow Area (from sketch)	Ground squirrel, *Spermophilus brunneus*	9.12E+02	cm^2
Soil Creep		***Measurement ID***	***Measurement interval***		
12	Fleming and Johnson, 1975	S11	1.17 yrs	3.76E+00	cm
13		S12	1.18 yrs	1.67E+00	cm
14		S18	1.14 yrs	1.02E+00	cm
15		S19	0.89 yrs	9.14E-01	cm
16		S20	1.14 yrs	1.02E+00	cm
17	Kirkby, 1967	Bluff	1-2 yrs	1.33E-01	$cm\ yr^{-1}$
18		Peat	1-2 yrs	1.10E-01	$cm\ yr^{-1}$
19		Rock	1-2 yrs	3.13E-01	$cm\ yr^{-1}$
20		Till	1-2 yrs	1.54E-01	$cm\ yr^{-1}$
21	Lewis, 1976	Marimonte	5.4 yrs	2.50E+01	cm
22		Infiernillo	4.4 yrs	1.70E+01	cm
23		Coama	5.4 yrs	2.54E+01	cm
24		LaPaguera	4.4 yrs	1.50E+01	cm
25		Piedra	4.4 yrs	1.34E+01	cm
26	Moeyersons, 1988		4 yrs	1.50E+00	cm

Figure S1A

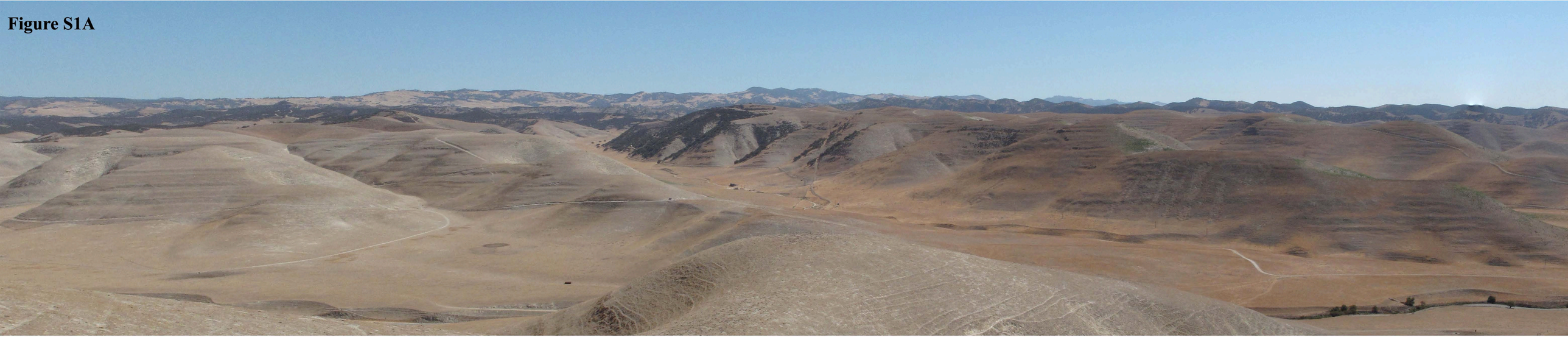

B

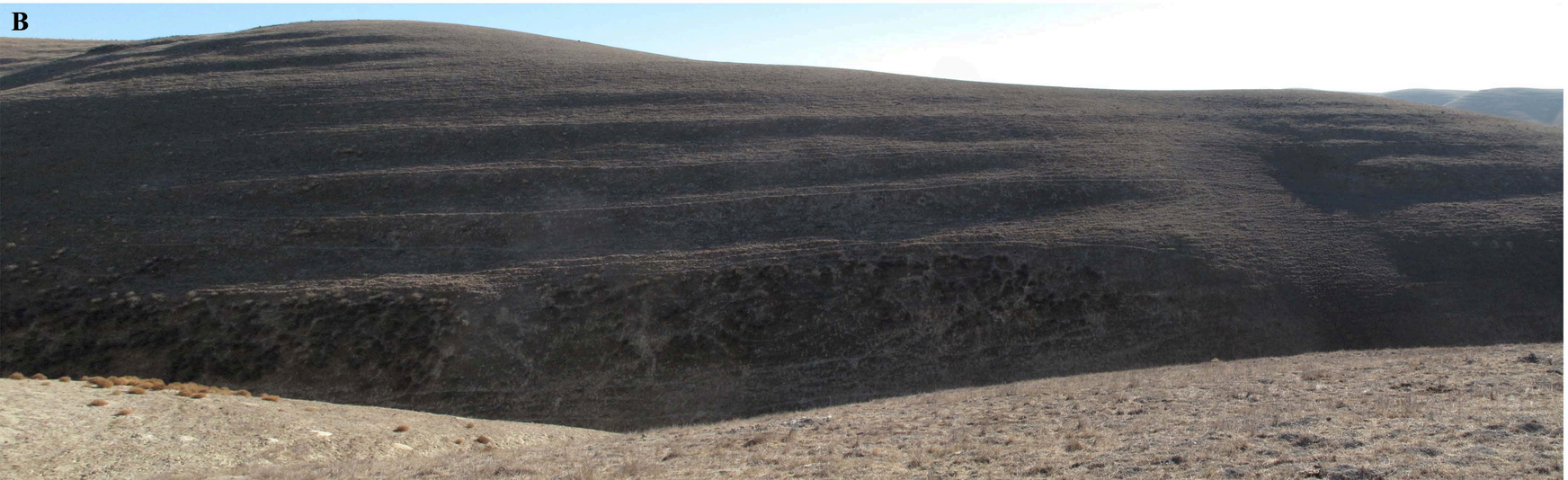

C

Figure S2

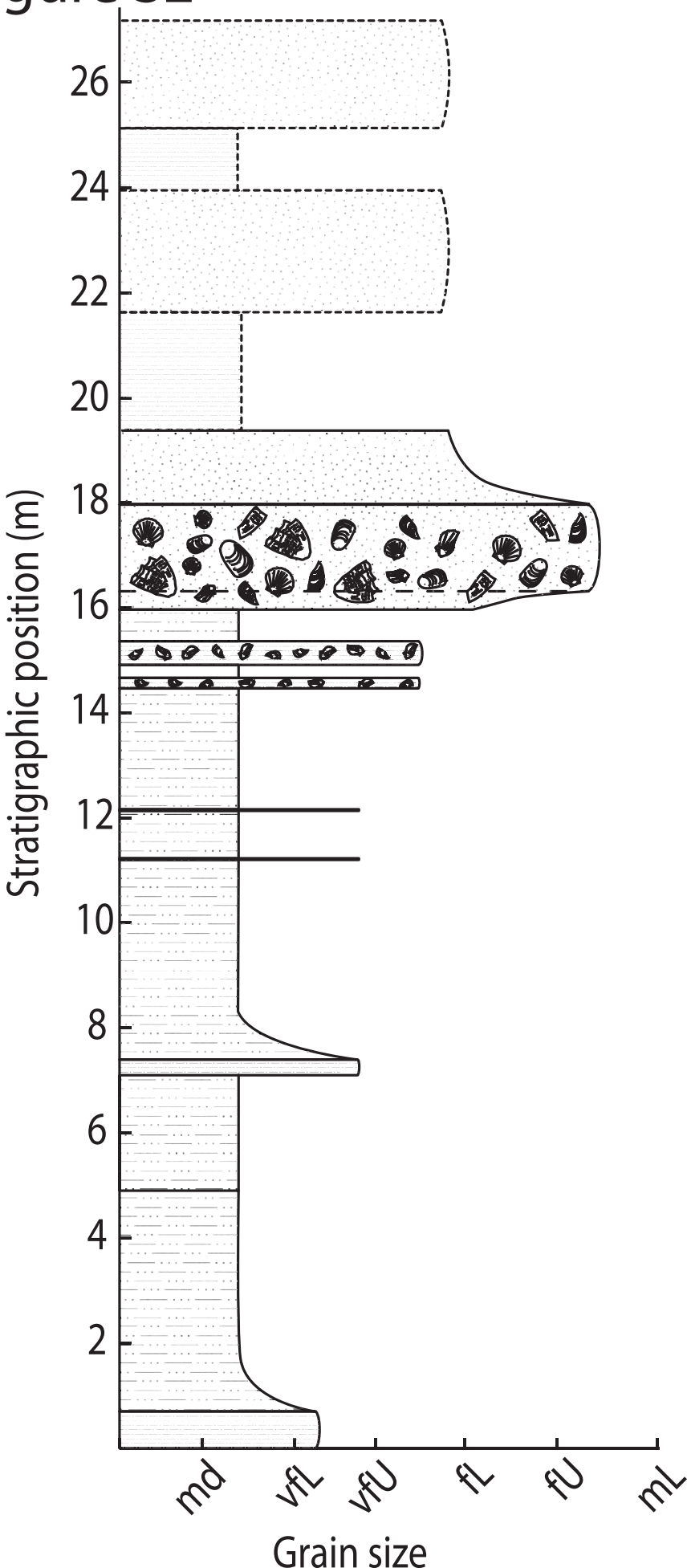
Stratigraphic position (m)
26
24
22
20
18
16
14
12
10
8
6
4
2
md
vfL
vfU
fL
fU
mL
Grain size

Figure S3

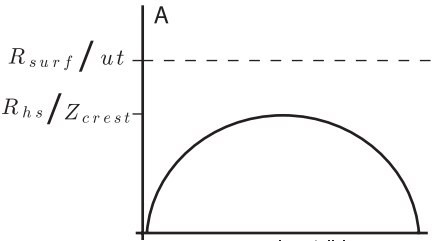

$$E^* = \frac{ut}{Z_{crest}} = \frac{R_{surf}}{R_{hs}}$$